EFFECTS OF PREGNANCY ON COLLAGEN MICROSTRUCTURAL ORGANIZATION OF HUMAN CERVICAL TISSUE

A Thesis

Presented to the Faculty of the Graduate School

of Cornell University

in Partial Fulfillment of the Requirements for the Degree of

Master of Science

by

Jia Hao

August 2017

ABSTRACT

BACKGROUND The cervix shortens and softens as its collagen microstructure rearranges (termed “remodeling”) in preparation for birth. Altered cervical tissue microstructure can contribute to premature cervical dilation and delivery. To date, the changes in cervical microstructure during pregnancy are poorly understood, and a quantitative comparison of collagen distribution and orientation within the cervix at the micron-scale is lacking.

OBJECTIVE To investigate the local microstructural changes associated with pregnancy and anatomic location, we quantitatively characterized the orientation and spatial distribution of collagen throughout human cervical tissue using second harmonic generation (SHG) microscopy.

STUDY DESIGN Using institutional review board-approved protocols, pregnant and non-pregnant women <50 years old undergoing hysterectomy for benign indications were consented. To characterize cervical microstructure throughout the entire cervix, cervical slices were obtained from the upper, middle, and lower cervix. We imaged samples excised at different anatomic locations using SHG microscopy and implemented a 2D autocorrelation method to quantify the microstructural orientation and distribution of collagen fibers. The effect of several obstetric history variables on collagen microstructure was examined: pregnancy status, parity, and number of vaginal deliveries. Student’s *t*-tests or Wilcoxon rank-sum tests and one-way ANOVA were used to examine differences across groups, and linear regression were used to examine relationships among variables.

RESULTS Cervical tissue was collected from 4 pregnant and 14 non-pregnant women. Collagen fibers of cervical samples from pregnant women are more disordered on the 90 μm-length scale, while cervical tissue from non-pregnant women have an 8% higher degree of orientation on this length scale. Collagen alignment trended toward decreasing as parity increases. Cervical collagen alignment was variable near internal os, and less variable near external os. Cervical tissue located at the inner radial zone (near the inner canal of cervix) are more homogeneously distributed than tissue located at the outer radial. Two regions with different collagen distribution characteristics were found. Cervical tissue at region 1 (anterior and posterior quadrants at outer radial) are more heterogeneously distributed than other regions.

Key words: cervix, collagen microstructure, premature cervical remodeling, preterm birth, SHG imaging

BIOGRAPHICAL SKETCH

Jia completed her undergraduate studies in the Materials Science and Engineering department at University of Science and Technology Beijing in June 2015. She then started researching collagen microstructure in Dr. Eve Donnelly's laboratory in the fall of 2015 at Cornell to pursue an M.S degree. After completing her master's degree, Jia will enter the Ph.D. program in Biomedical Engineering at University of Southern California.

ACKNOWLEDGEMENTS

I would like to thank my advisor, Dr. Eve Donnelly, for her guidance and support throughout the time I have worked in her laboratory. The members of the Donnelly research group, Heather Hunt, Ashley Lloyd, Pablo Palomino and Erik Taylor, were always eager to discuss my research and challenge my thinking. Dr. Rebecca Williams and Dr. Johanna Dela-Cruz were ever patient in assisting with the technical operation of the SHG microscope. I would also like to thank Dr. Kristin Myers, Dr. Joy Vink and Dr. Frank Yao at Columbia University for collecting and preparing samples used in these experiments, and for valuable discussions of the results.

TABLE OF CONTENTS

LIST OF TABLE AND FIGURES

INTRODUCTION

Preterm birth (PTB) poses a worldwide, significant problem to both patients and doctors with an increased risk of perinatal death and a litany of associated long-term morbidities. Depending on the country of origin, the frequency of babies born before 37 weeks' gestation can range from 7-15% of total births (Goldenberg et al., 2008). Understanding physiologic changes over the course of pregnancy will enable discovery of proper diagnostic and preventative measures for preterm birth.

Cervical tissue is comprised (34-77% dry weight) of type I and type III collagen embedded in a ground substance that contains hydrated glycosaminoglycans and hyaluronic acid (Myers et al., 2009). Cervical remodeling in animal models is achieved in part by a decline in collagen cross-link formation, a reduction in matricellular proteins that regulate collagen fibrillogenesis, and increased synthesis of the matrix disorganizing molecule, hyaluronan (Ruscheinsky et al., 2008; Yoshida et al., 2014). The progressive structural changes in fibrillar collagens are directly related to cervical material properties and thus potentially can serve as a diagnostic indicator for women at risk for PTB. (Zhang et al., 2012)

Cervical remodeling with pregnancy is reflected in changes in collagen alignment. Specifically, non-pregnant cervices contain three zones of collagen fibers aligned radially around the central canal (Weiss et al., 2006) In contrast, immediately after delivery, the cervix's collagen fibers no longer have preferred alignment and are randomly oriented (Aspden et al., 1988). Furthermore, the collagenous network of the cervical stroma was anisotropic, and pregnancy was associated with a discernable decrease in collagen organization (Myers et al., 2009). Preliminary SHG studies

(Feltovich et al., 2013) revealed a large band of circumferential fibers extending to the outer edge of the tissue. There are two radially zones with distinct fiber orientation characteristics at the internal os of non-pregnant cervical tissue, an inner zone with collagen fibers preferentially aligned in the radial direction and an outer zone with collagen fibers preferentially aligned in the circumferential direction. The posterior and anterior of the outer radial zone of non-pregnant specimens have also been shown to have the lowest collagen dispersion. (Yao, Gan, Myers, Vink, & Wapner, 2016)

Despite considerable evidence of differing microstructures between pregnant and non-pregnant cervices, the collagen microstructures of pregnant and non-pregnant human cervices have not yet been quantitatively characterized. The knowledge that could be gained from such a comparison includes a better understanding of structure-function relationships, which could ultimately help describe the differences between characteristic structural properties of pregnant and non-pregnant cervices and explain how human cervical tissue remodels during pregnancy. Therefore, our objective is to characterize the microstructure of human cervical tissue throughout the entire cervix to better understand differences in microstructure between pregnant and non-pregnant cervices. Specifically, we quantitatively compared the collagen fiber orientation and distribution in pregnant and non-pregnant cervical tissue throughout the entire cervix using second harmonic generation (SHG) microscopy. We hypothesized that collagen in tissue from pregnant patients would be more disordered than that from non-pregnant patients.

MATERIALS AND METHODS

Sample collection and preparation

Eighteen human cervices were collected from consented hysterectomy patients by an IRB approved protocol at Columbia University Medical Center and patient obstetric history is recorded (Table 1). Among the cervices, 14 were from non-pregnant (NP) patients undergoing hysterectomy for benign indications and 4 were from pregnant (PG) patients undergoing cesarean hysterectomy due to abnormal placentation. Patient ages range from 24 to 49 and parity number from 0 to 4. The cervix was excised from the uterus and sectioned perpendicular to the inner canal, in six slices (Figure 1). Slice 1 is the most superior and slice 6 is the most inferior with respect to the cervix. Eight-mm-diameter biopsies were then taken from different circumferential quadrants located at inner and outer radial zones of each cervical slice and stored at -80°C in optimal cutting temperature compound (Sakura Finetek USA, Inc., Torrance, CA).

SHG microscopy

Prior to SHG imaging, cervical samples were thawed, rinsed five times in NaCl buffer (2 mol/L), and left to equilibrate overnight in fresh buffer at 4°C. SHG microscopy was used to acquire images of the collagen microstructure. SHG occurs when pulsed light reacts simultaneously with the non-centrosymmetric structure of the collagen, scattering photons at twice the energy of the incident beam (Williams, Zipfel, & Webb, 2005). This technique allows for optical sectioning, subsurface visualization, and the use of relatively benign near-infrared laser light energies (Zipfel, Williams, & Webb, 2003). A second-harmonic signal was generated using a Mai Tai laser (Mai Tai DeepSee, Spectra-Physics, Mountain View, CA) providing a pulse width of less than

100 fs at a 780-nm wavelength.

The incident beam was circularly polarized using a Berek variable waveplate (5540, New Focus, San Jose, CA). Imaging was performed with a laser scanning confocal microscope ZEISS LSM 880 Upright (Carl Zeiss, Oberkochen, Germany). For each sample, a large representative 2427.7 μm x 2427.7μm region from the center of the biopsy was imaged using a 5x 0.25 Fluar objective lens (Carl Zeiss, Oberkochen, Germany) with a digital zoom of 0.7x. Within the large region, three 92.4 μm x 92.4 μm regions of interest (ROIs) were randomly selected for detailed imaging using a 20x 0.75 NA Fluar objective lens (Carl Zeiss, Oberkochen, Germany) with a digital zoom of 4.7x. If an initially selected ROI fell on a large hole, a new ROI was randomly selected. At each ROI, a z-stack was acquired using 1-μm z-increments beginning at the surface of the biopsy until no signal was detectable.

Image analysis

Image analysis was performed on the central 14μm (15 slices) of each image stack. The surface images were excluded to avoid possible tissue damage on surfaces of the biopsies that occurred during excision, and the bottom images were excluded due to signal attenuation. A custom 2D autocorrelation program (IDL, Exelis Visual Information Solutions, Inc., Boulder, CO) was used to perform the analysis (Schwille & Haustein, n.d.). For each z-stack image, a 2D autocorrelation array was generated to describe the spatial similarities within the image and normalized to the maximum intensity (Figure 2B). A 2D Gaussian surface was fit to the normalized autocorrelation array G (Figure 2C), and two key parameters were calculated to describe the collagen microstructure: the heterogeneity of intensity (G_0) and the Ellipticity. The G_0 term is calculated as the

maximum value of the fitted Gaussian surface (Figure 2C), with a higher G_0 corresponding to greater variation in intensity within an image. Physically, the G_0 term relates to the concentration of aligned collagen because the SHG intensity scales with the square of the number of aligned molecules (Moreaux, Sandre, & Mertz, 2000). A high G_0 value indicates an imaged region contains both aligned collagen and unaligned and/or missing collagen. Ellipticity is calculated as the ratio of major to minor axes of an ellipse fit to the Gaussian surface at a height of $0.5G_0$ (Figure 2C, D). Ellipticity describes the alignment of the collagen fibers, with higher values corresponding to greater collagen alignment, and values closer to 1 corresponding to disordered collagen fibers.

Statistical analysis

Ellipticity and heterogeneity of intensity measured at each of the three ROIs per biopsy were averaged to obtain a single value for each sample, and outcomes of samples taken from the same patient were averaged to obtain a single value for each patient. Student's t tests or Wilcoxon tests (JMP, Cary, NC) were used examine differences in microstructural parameters between groups as a function of obstetric history variables (pregnancy status and number of vaginal deliveries) and as a function of anatomic locations within the cervix (quadrant, radial zone and slice number). Microstructural parameters were examined as a function of position within the cervix from internal os (slice 1) to external os (slice 6), anatomic quadrant, and parity groups using one-way ANOVA. Tukey-Kramer HSD was used for comparisons for pairs. The data normality was tested by Kolmogorov-Smirnov tests (JMP, Cary, NC). Relationships between the microstructural outcomes and predicting variables including obstetric history variables and anatomic variables (Table 2) were examined using linear

regressions. For all analyses, $p < 0.05$ was considered significant.

RESULTS

The collagen microstructure was quantified using two parameters: ellipticity, which assesses the collagen alignment, and the heterogeneity of intensity (G_0), which assesses the extent to which the concentration of aligned collagen varies within an image. When collagen microstructural parameters were examined as a function of obstetric history variables, the largest difference was observed when patients were grouped by pregnancy status. Specifically, collagen alignment as assessed by ellipticity of the collagen matrix trended toward being lower in cervical tissue of women who were pregnant compared to women who were non-pregnant (-8%, p = 0.0773) (Figure 3A). Ellipticity also trended toward decreasing as parity increased (p = 0.0960 by ANOVA) (Figure 3B). Although the ellipticity was 15% higher in the group of parity = 0 than the group of parity > 1, this difference did not reach statistical significance. Ellipticity was similar across groups with different histories of vaginal deliveries (Figure 3C). The heterogeneity of intensity (G_0) was similar across tissue from all obstetric groups (Figure 3D, E, F).

Next, variation in microstructural variables were examined as a function of position from upper to lower cervix (Figure 1A). Collagen alignment as assessed by ellipticity was highly variable in tissue near internal os (slice 1, COV = 0.2436) and less variable near external os (slice 6, COV = 0.0725) (Figure 4A). Overall, the average values of ellipticity and heterogeneity of intensity (G_0) were similar with position from upper to lower cervix (Figure 4A, B).

When samples were grouped based on anatomic location with respect to the central canal (taken from inner radial or outer radial zone of the cervix, Figure 1D), samples located at the inner radial zone had lower heterogeneity of intensity (G_0) than samples taken from the outer radial zone (-20%, p=0.0460) (Figure 5B). No difference in

ellipticity was observed between samples from these groups (Figure 5A). Microstructural variables were also compared between two anatomic regions within the cervix, Region 1 (anterior and posterior quadrants at outer radial zone) and Region 2 (other quadrants in outer radial and all inner radial zone). These regions have been reported to vary in collagen dispersion and sensitivity to cervical remodeling during pregnancy (Wang Yao et al., 2016). Tissue from Region 1 trended toward having higher heterogeneity of intensity (G_0) than Region 2 (+33%, $p = 0.0659$) (Figure 5D), but had similar ellipticity (Figure 5C). When microstructural parameters were examined as a function of anatomic quadrants (anterior, posterior, right), no difference was observed in ellipticity or heterogeneity of intensity (G_0) (Figure 5E, F).

When relationships between microstructural variables and predictors such as obstetric history variables and anatomic variables (Table 2) were examined, the single best predictor of ellipticity was parity. Specifically, ellipticity trended toward decreasing as parity increased ($R^2 = 0.28$, $p = 0.0960$). No other obstetric history variables were significant explanatory variables for the microstructural parameters examined. However, anatomic variables were significant explanatory variables for the microstructural parameters. Heterogeneity of intensity (G0) increased from inner radial zones to outer radial zones ($R^2 = 0.29$, $p = 0.0298$, but a similar effect on ellipticity was not observed. No other anatomic variables were significant explanatory variables for the microstructural parameters examined.

DISCUSSION

The objectives of this study were to investigate the effect of pregnancy on collagen microstructural organization of human cervical tissue. Two microstructural parameters

were examined in cervical tissue from 14 non-pregnant patients and 4 pregnant patients as a function of obstetric history variables as well as anatomic locations.

Our findings suggest that the collagen alignment of cervical tissue varies among women with different obstetric histories. Collagen in cervical tissue from pregnant women trended toward having overall less collagen alignment than non-pregnant women. Collagen in cervical tissue from women with greater parity trended toward having decreased alignment.

In addition, collagen microstructural organization also differs among anatomic locations. We also found that collagen alignment was highly variable in tissue near the internal os, which contains 50-60% cervical smooth muscle cells, and less variable near the external os, which contains only 10% cervical smooth muscle cells (Vink et al., 2016). The internal os has been suggested to be the anatomic structure most essential to normal cervical function by both magnetic resonance imaging (MRI) and ultrasound (US) imaging (Myers et al., 2015). Our study suggests that this difference in collagen microstructural alignment may reflect local anatomic differences in cervical function.

Cervical tissue in the outer radial zone was characterized by greater spatial heterogeneity of aligned collagen than that of the inner radial zone. In particular, the anterior and posterior sections in the outer radial zone (Region 1) were characterized by greater spatial heterogeneity of aligned collagen than that of the rest of sections (Region 2). These regions have been reported to vary in collagen dispersion assessed by optical coherence tomography (OCT), where Region 1 was found to be more oriented at the millimeter length scale than Region 2 (Yao et al., 2016). These region-specific differences in structural organization may reflect an adaptive response to the local mechanical

environment of the cervix. In pregnancy, the cervical axis is angled posteriorly from the uterine axis. This positioning leads to increased tissue loads and stretching in the anterior and posterior sections of the cervix (Fernandez et al., 2016), and contributes to the difference in collagen distribution between Region 1 and Region 2.

This study has key limitations and strengths. Limitations of this study included that pregnant samples were taken from term patients with placenta accreta and may therefore not reflect normal remodeling. Additionally, the sample size of the pregnant patients is relatively small (N = 4), which limits the generalizability of the data. Also, our SHG imaging was only conducted on transverse two-dimensional slices of cervix. The microstructural collagen organization along the central canal was not studied. The key strength of this study is the use of both pregnant and non-pregnant human cervical tissue. Most previous studies in cervical remodeling were conducted on mouse cervices.

This study also demonstrated that second harmonic generation microscopy is a promising approach to quantitatively evaluate the microstructure of human cervical tissue to assess premature remodeling. With the development and prevalence of SHG imaging for clinical endoscopy (Zhang et al., 2012), Collagen alignment, as assessed by ellipticity, shows potential as a next generation diagnostic marker of cervical remodeling, with decreased collagen alignment associated with pregnancy and greater parity. Furthermore, in the future, the effect of pregnancy on other matrix components that affect cervical softening will be studied, including alignment and distribution of smooth muscle cells and acellular components at different anatomic locations throughout the cervix. Three-dimensional studies of collagen microstructural distribution would also be valuable due to the complexity of the structure of the human cervix. In combination with studies from

organ level to molecular level, ultimately, a comprehensive understanding of specific cervical change in pregnancy should facilitate targeted exploration of associated molecular mechanisms and lead to novel therapies for preterm birth.

REFERENCES

Aspden, R. M. (1988). Collagen Organisation in the Cervix and its Relation to Mechanical Function. *Collagen and Related Research Clinical and Experimental*, *8*(2), 103–112. https://doi.org/10.1016/S0174-173X(88)80022-0

Moreaux, L., Sandre, O., & Mertz, J. (2000). Membrane imaging by second-harmonic generation microscopy. *Journal of the Optical Society of America B*, *17*(10), 1685. https://doi.org/10.1364/JOSAB.17.001685

Myers, K. M., Feltovich, H., Mazza, E., Vink, J., Bajka, M., Wapner, R. J., … House, M. (2015). The mechanical role of the cervix in pregnancy. *Journal of Biomechanics*, *48*(9), 1511–1523. https://doi.org/10.1016/j.jbiomech.2015.02.065

Ruscheinsky, M., De la Motte, C., & Mahendroo, M. (2008). Hyaluronan and its binding proteins during cervical ripening and parturition: dynamic changes in size, distribution and temporal sequence. *Matrix Biology: Journal of the International Society for Matrix Biology*, *27*(5), 487–97. https://doi.org/10.1016/j.matbio.2008.01.010

Schwille, P., & Haustein, E. (n.d.). Fluorescence Correlation Spectroscopy An Introduction to its Concepts and Applications, 1–33.

Vink, J. Y., Qin, S., Brock, C. O., Zork, N. M., Feltovich, H. M., Chen, X., … Gallos, G.

(2016). A new paradigm for the role of smooth muscle cells in the human cervix. *The American Journal of Obstetrics & Gynecology*, (May), 1–11. https://doi.org/10.1016/j.ajog.2016.04.053

Weiss, S., Jaermann, T., Schmid, P., Staempfli, P., Boesiger, P., Niederer, P., … Bajka, M. (2006). Three-Dimensional Fiber Architecture of the Nonpregnant Human Uterus Determined Ex Vivo Using Magnetic Resonance Diffusion Tensor Imaging, *90*(October 2005), 84–90. https://doi.org/10.1002/ar.a.20274

Williams, R. M., Zipfel, W. R., & Webb, W. W. (2005). Interpreting second-harmonic generation images of collagen I fibrils. *Biophysical Journal*, *88*(2), 1377–1386. https://doi.org/10.1529/biophysj.104.047308

Yao, W., Gan, Y., Myers, K. M., Vink, J. Y., & Wapner, R. J. (2016). Collagen Fiber Orientation and Dispersion in the Upper Cervix of Non-Pregnant and Pregnant Women, 1–21. https://doi.org/10.1371/journal.pone.0166709

Yoshida, K., Jiang, H., Kim, M. J., Vink, J., Cremers, S., Paik, D., … Myers, K. (2014). Quantitative evaluation of collagen crosslinks and corresponding tensile mechanical properties in mouse cervical tissue during normal pregnancy. *PLoS ONE*, *9*(11), 1–11. https://doi.org/10.1371/journal.pone.0112391

Zhang, Y., Akins, M. L., Murari, K., Xi, J., Li, M., & Luby-phelps, K. (2012). A compact fiber-optic SHG scanning endomicroscope and its application to visualize cervical remodeling during pregnancy, *109*(32), 12878–12883. https://doi.org/10.1073/pnas.1121495109

Zipfel, W. R., Williams, R. M., & Webb, W. W. (2003). Nonlinear magic: multiphoton

microscopy in the biosciences. *Nature Biotechnology*, *21*(11), 1369–1377. https://doi.org/10.1038/nbt899

Figure legends

Figure 1. Methods utilized in this study. A, E) Cervix slices were excised from internal os to external os and numbered from slice 1 to 6. B, F) 8 mm samples were punched within each slice. SHG microscopy is used to image the samples in z axis. C) Illustration of two radial zones and quadrants. A = anterior, P = posterior, L = left, R = right. Red is inner radial zone; pink is outer radial zone. D) Illustration of two anatomic regions. Red is Region 1; pink is Region 2. Representative images of collagen microstructure are shown at G) 2427.7 μm x 2427.7μm, scale bar = 500 um and H) 92.4 μm x 92.4 μm, scale bar = 30μm.

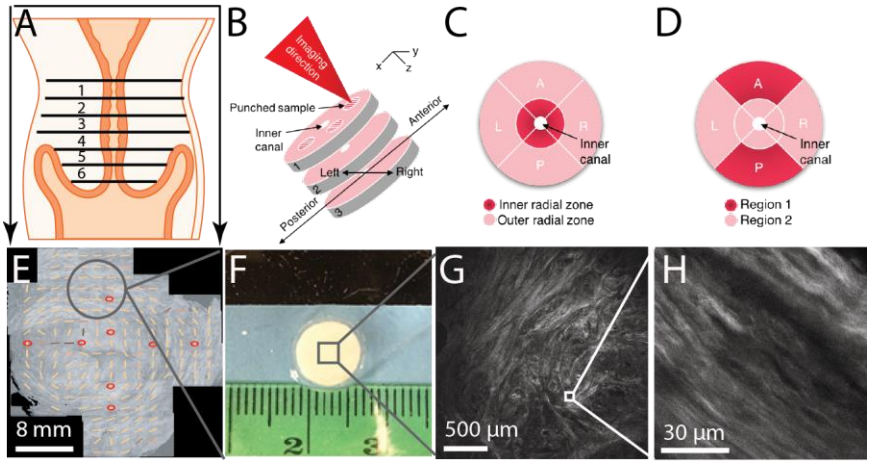

Figure 2. Illustration of 2D autocorrelation and calculation of collagen microstructure parameters. A) SHG image, input for 2D autocorrelation (scale bar = 30μm). B) Map of pixel intensity from 2D autocorrelation. C) 2D Gaussian fit of the pixel intensity map. Blue ellipse = ellipse fit at ½ of the maximum G value, Red point = G_0 (z axis) D) Ellipse mapped on 2D coordinates (250 x 250 pixel).

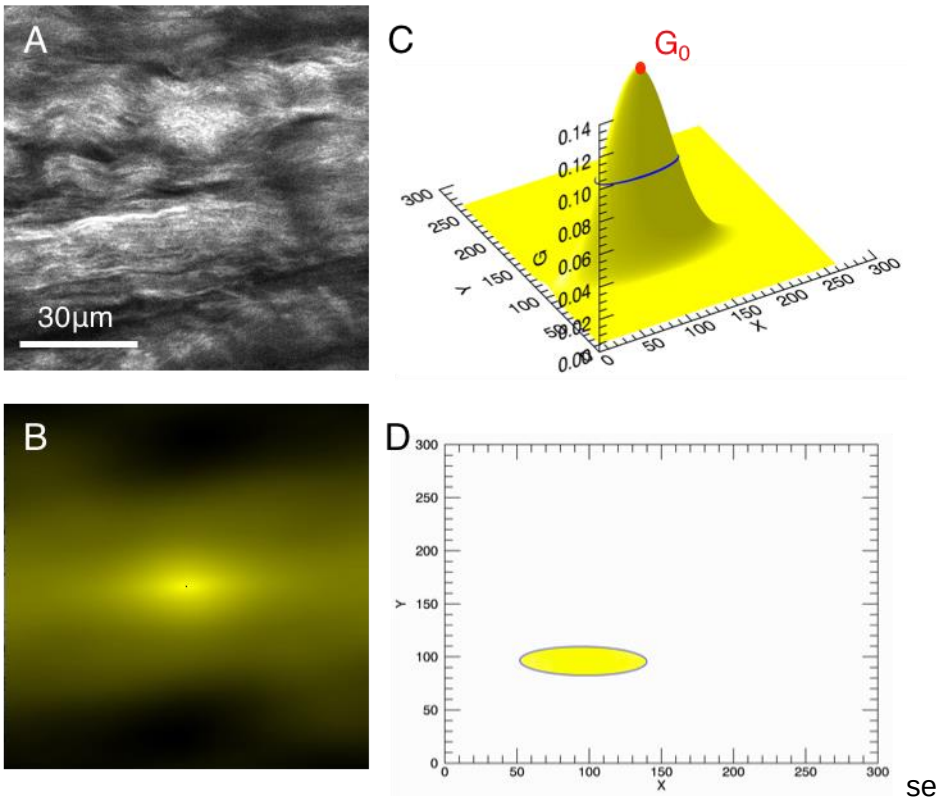

se

Figure 3. Cervical tissue microstructure parameters ellipticity and heterogeneity of intensity (G_0) shown as a function of obstetric history variables (N=18). A) Ellipticity vs. Pregnancy Status. NP = Non-pregnant, PG = Pregnant. B) Ellipticity vs. Parity groups. P = Parity. C) Ellipticity vs. Vaginal deliveries. VD = Vaginal deliveries. D)Heterogeneity of intensity (G_0) vs Pregnancy status. E) Heterogeneity of intensity (G_0) vs. Parity groups. F) Heterogeneity of intensity (G_0) Vaginal deliveries. # = $p<0.10$ by Wilcoxon rank sums (A) or ANOVA (B).

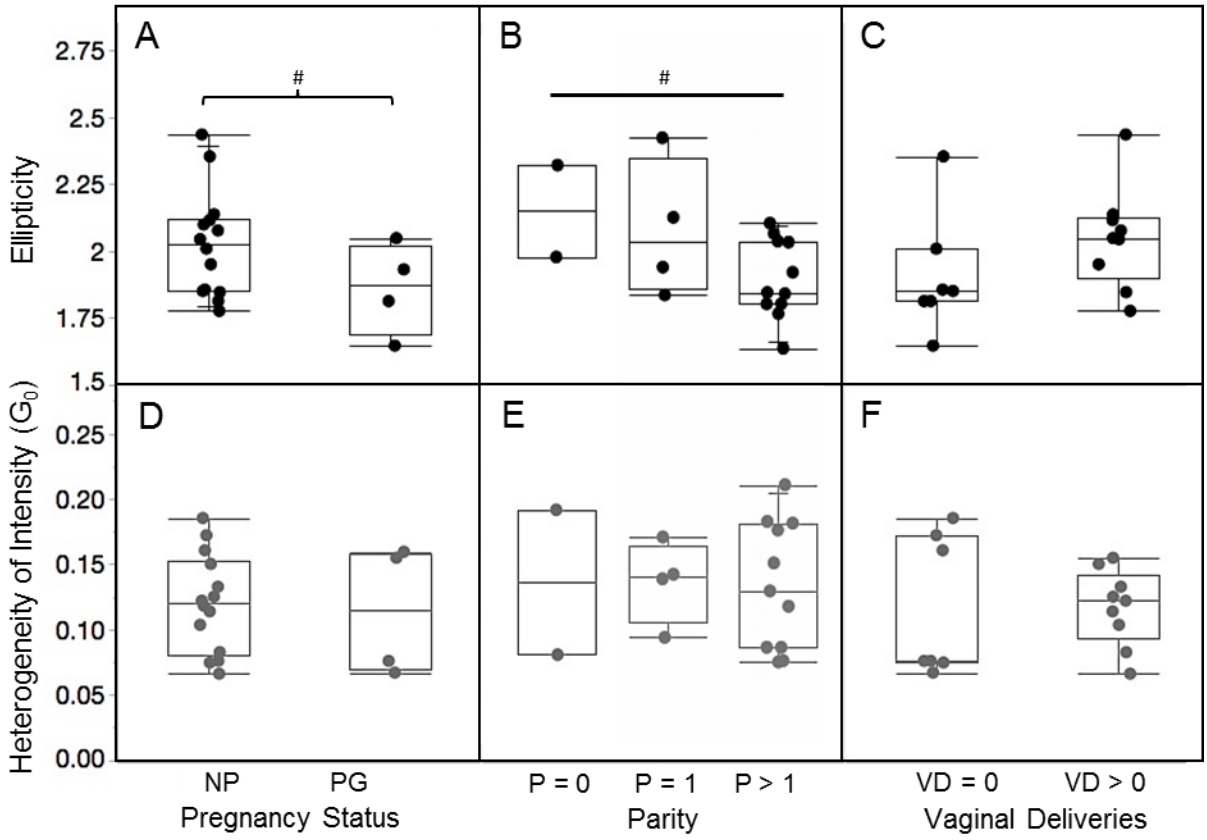

Figure 4. Cervical tissue microstructure parameters ellipticity and heterogeneity of intensity (G_0) shown as a function of slice number (slice 1 is internal os; slice 6 is external os) (N=36). A) Ellipticity vs. Slice no. B) Heterogeneity of intensity (G_0) vs. Slice no.

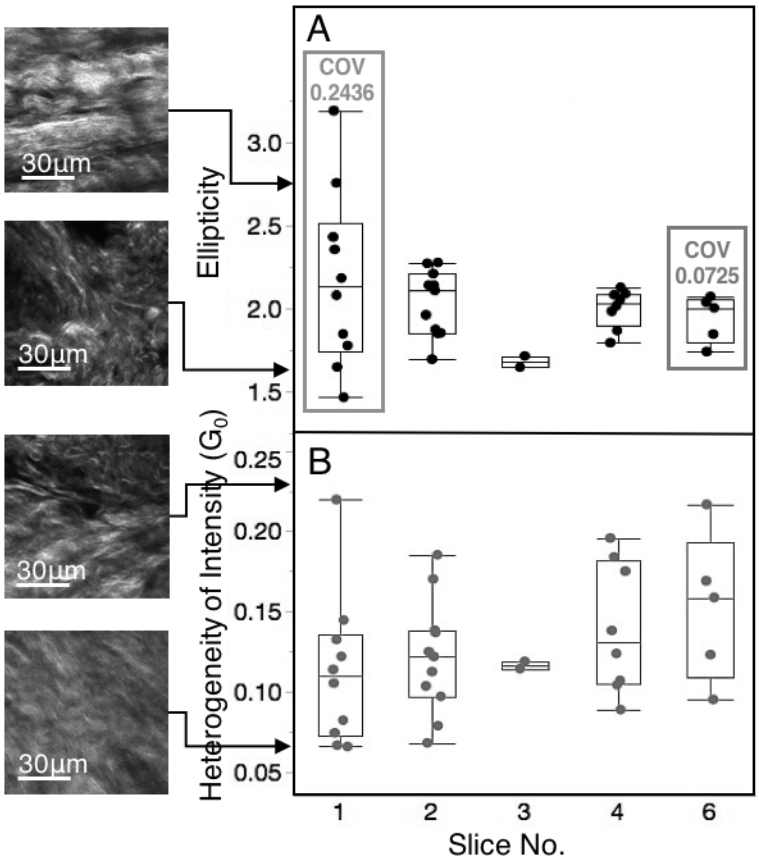

Figure 5. Collagen microstructure parameters ellipticity and heterogeneity of intensity (G_0) shown as a function of anatomic regions (N = 16). Region 1 includes anterior and posterior quadrants of outer radial zone. Region 2 comprises all other outer radial and all inner radial zones (Figure 1D). A) Ellipticity vs. Radial zone. B) Heterogeneity of intensity (G_0) vs. Radial zone. C) Ellipticity vs. Anatomic region. D) Heterogeneity of intensity vs. Anatomic region. E) Ellipticity vs Quadrant. A = Anterior, P = Posterior, R = Right. F) Heterogeneity of intensity (G_0) vs. Quadrant. * = $p < 0.05$, # = $p < 0.10$ by student's *t* test or Wilcoxon rank sums.

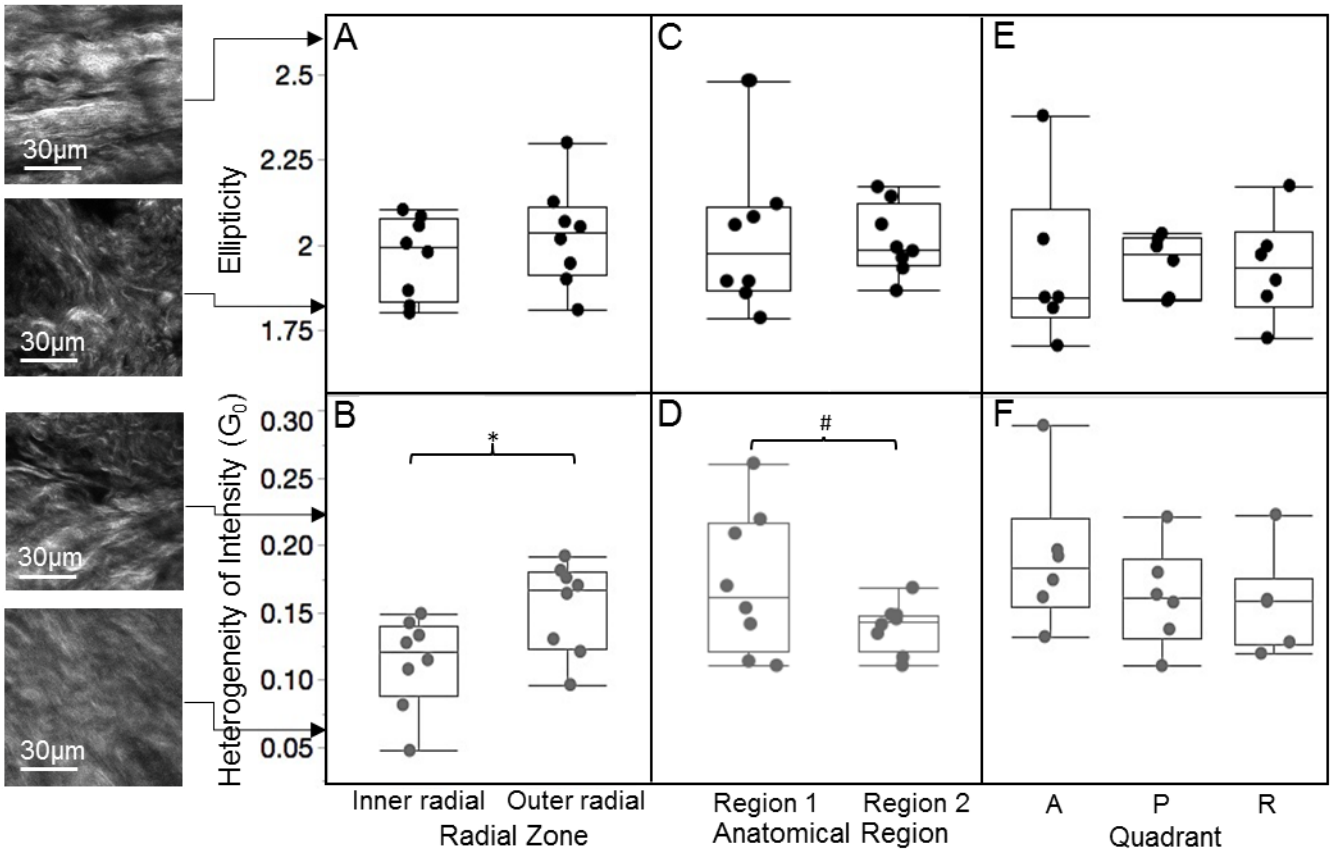

TABLE 1

Patients demographics for cervical tissue

Patient no.	Collection Date	Age, y	Previous pregnancies G/TPAL	Obstetric History	# Slices analyzed
PG1	12/16/14	42	5/2022		2
PG2	10/22/12	29	4/3013	3 CS	1
PG3	4/6/12	35	3/2002	1 VD, 1 CS	4
PG4	12/14/11	24	6/4014	4 CS, 1 SAB	1
NP1	9/29/14	46	0/0000		3
NP2	8/21/14	43	1/1001	1 VD	2
NP3	8/25/14	49	1/1001	1 VD	1
NP4	2/19/14	42	51041	1 VD, 3 VTOP	3
NP5	9/24/14	40	3/3003	3 VD	2
NP6	9/25/14	36	4/4004	4 CS	3
NP7	2/24/14	41	6/4024	4 VD, 1 VTOP, 1 SAB	4
NP8	7/14/11	41	4/2022	2 CS, 1 VTOP, 1 SAB	1
NP9	10/05/11	44	3/3003	1 VD, 2 CS	1
NP10	3/9/12	38	3/2002	2 CS	1
NP11	3/15/12	46	2/1011	1 VD, 1 SAB	4
NP12	4/16/12	-	-	-	2
NP13	9/7/12	36	0/0000		1

NP14	11/25/13	38	3/2014	2 VD, 1 VD twins	1

Patient no.: PG = pregnant, NP, non-pregnant.

G/TPAL: G = gravidity (total number of pregnancies), TPAL = term, preterm, aborted, and living deliveries in the order of the four digits.

Obstetric history: VD = vaginal delivery, CS = cesarean section, VTOP = voluntary termination, SAB = spontaneous abortion.

Anatomic locations: SL = slice number; A = anterior, P = posterior, R = right; I = inner radial, O = outer radial.

TABLE 2 Variables used for linear regressions.

Variable	**Category**	**Values**
Ellipticity	Continuous	
G_0	Continuous	
Slice no.	Ordinal	0-slice 1; 1-slice 2; 2-slice 3; 3-slice 4; 4-slice 6.
Parity	Ordinal	parity = 0; parity = 1; parity > 1
Vaginal deliveries	Ordinal	0-VD = 0; 1-VD = 1; 2-VD >1.
Pregnancy status	Nominal	0-NP; 1-PG.
Anatomic region	Nominal	0-Region 1; 1-Region 2.
Radial zone	Nominal	0-Inner radial zone; 1-Outer radial zone.